European Journal of Immunology

Immunity to infection

Basic

Research Article

MHC I presentation of *Toxoplasma gondii* immunodominant antigen does not require Sec22b and is regulated by antigen orientation at the vacuole membrane

Célia Buaillon[*1], *Nestor A. Guerrero*[*1], *Ignacio Cebrian*[2], *Sophie Blanié*[1], *Jodie Lopez*[1], *Emilie Bassot*[1], *Virginie Vasseur*[1], *Julien Santi-Rocca*[1] *and Nicolas Blanchard*[1]

[1] Centre de Physiopathologie Toulouse Purpan (CPTP), INSERM, CNRS, Université de Toulouse, UPS, Toulouse, France
[2] Instituto de Histología y Embriología de Mendoza (IHEM)-CONICET/UNCuyo, Facultad de Ciencias Médicas, Universidad Nacional de Cuyo, Mendoza, Argentina

The intracellular *Toxoplasma gondii* parasite replicates within a parasitophorous vacuole (PV). *T. gondii* secretes proteins that remain soluble in the PV space, are inserted into PV membranes or are exported beyond the PV boundary. In addition to supporting *T. gondii* growth, these proteins can be processed and presented by MHC I for CD8$^+$ T-cell recognition. Yet it is unclear whether membrane binding influences the processing pathways employed and if topology of membrane antigens impacts their MHC I presentation. Here we report that the MHC I pathways of soluble and membrane-bound antigens differ in their requirement for host ER recruitment. In contrast to the soluble SAG1-OVA model antigen, we find that presentation of the membrane-bound GRA6 is independent from the SNARE Sec22b, a key molecule for transfer of host endoplasmic reticulum components onto the PV. Using parasites modified to secrete a transmembrane antigen with opposite orientations, we further show that MHC I presentation is highly favored when the C-terminal epitope is exposed to the host cell cytosol, which corresponds to GRA6 natural orientation. Our data suggest that the biochemical properties of antigens released by intracellular pathogens critically guide their processing pathway and are valuable parameters to consider for vaccination strategies.

Keywords: Antigen cross-presentation · Dendritic cell · Intracellular pathogen · MHC I presentation · Parasite · *Toxoplasma gondii*

Additional supporting information may be found in the online version of this article at the publisher's web-site

Introduction

Toxoplasma gondii (*T. gondii*) is the causative agent of toxoplasmosis, an opportunistic disease with potential deadly consequences for immunocompromised individuals and congenitally infected newborns [1]. *T. gondii* also constitutes an emerging threat since outbreaks caused by virulent strains in South-America have killed non-immunocompromised humans [2]. CD8$^+$ T cells are critical for protection, both by limiting parasite replication during acute

Correspondence: Dr. Nicolas Blanchard
e-mail: nicolas.blanchard@inserm.fr

*These authors contributed equally to this work.

stage and by preventing encephalitis that follows reactivation of the persisting brain cysts [3–6]. $CD8^+$ T cells typically recognize 8–10 amino acid-long peptides presented by class I molecules of the major histocompatibility complex (MHC I). During *T. gondii* infection, MHC I antigenic peptides can theoretically be cross-presented either by parasite-infected cells or by cells that have internalized parasite debris. Given (i) that efficient MHC I presentation requires secretion of the antigen [7, 8] and (ii) that only infected dendritic cells (DCs) and not DCs that have phagocytosed the parasite, are able to prime naive $CD8^+$ T-cell responses [9], cross-presentation by actively infected cells is considered as the most relevant scenario. In mechanistic terms, MHC I processing was shown to be dependent on proteasome and TAP activity using the soluble SAG1-OVA model antigen [10, 11], suggesting that antigenic precursors may exit the PV and transit via the host cytosol. Entry into the cytosol is facilitated by fusion of vesicles from the host ER onto the PV [12] through a SNARE Sec22b-dependent mechanism [13]. By recruiting components of the ER-associated degradation (ERAD) machinery onto the PV membrane, this process, reminiscent of the ER-phagosome pathway [14, 15], is thought to allow retro-translocation of vacuolar antigens to the host cytosol and access to the MHC I pathway.

Beside the widely studied OVA model antigen, the identification of 'natural' antigens from *T. gondii*, including the immunodominant GRA6 antigen, shed new light on the mechanisms of protective T cell immunity during toxoplasmosis [16–21]. GRA6 is a protein secreted through the parasite dense granules in the vacuolar space. In the case of type II parasites, the decameric HPGSVNEFDF (HF10) peptide at GRA6 C-terminus is processed and presented by L^d MHC I molecules. Immunization with HF10 confers protection against lethal *T. gondii* challenge [16] and ectopic expression of HF10-containing GRA6 by type III *T. gondii,* that are naturally devoid of HF10 due to polymorphisms in GRA6 C-terminus, reduces parasite load [22]. Immune protection by HF10-specific $CD8^+$ T cells despite chronic persistence of the antigen involves the generation of a newly described proliferative population of memory-effector hybrid phenotype [20]. Yet the molecular mechanisms underlying the potent immunogenicity of GRA6 are only partially understood. Processing of GRA6 requires proteasome activity, TAP transport, ER aminopeptidase trimming [16] and the location of HF10 at the C-terminus [22] but whether host ER-PV interactions provide a route of entry for GRA6 cross-presentation remains unknown. An intriguing feature of GRA6 is that, like other dense granule proteins (e.g. GRA4 [23] and GRA5 [24]), it contains a hydrophobic domain that seems to be masked within the dense granules but inserts within the PV membranes following release, thereby making GRA6 an integral transmembrane protein (reviewed in [25]). In the PV, GRA6 scatters between the PV limiting membrane and an IntraVacuolar Network (IVN) of tubulovesicular membranes [26]. We recently found that membrane association properties of GRA6 strongly regulates its entry into the MHC I pathway since GRA6 presentation decreased when membrane association was disrupted and increased when GRA6 was relocalized from the IVN to the PV limiting membrane [27]. To this date however, the topology of GRA6 membrane insertion and whether it influences presentation of the C-terminal epitope, is unknown.

Here we determined to which extent host ER-PV fusion is involved in presentation of the membrane-bound GRA6 antigen. Using Sec22b-silenced DCs, we found no implication of this pathway in GRA6 presentation, contrary to the soluble SAG1-OVA antigen. Thanks to differential permeabilization assays, we established that the C-terminal HF10 epitope protrudes into the host cell cytosol. Using *T. gondii* engineered to express the HF10 epitope on GRA5, another transmembrane protein with an inverted topology, we observed a dramatic reduction in L^d-HF10 presentation by infected macrophages and DCs, suggesting a major impact of antigen orientation on processing efficiency.

Results

Presentation of GRA6 by infected DCs is independent of Sec22b

To determine if GRA6 processing requires recruitment of host ER material onto the PV, we analyzed the impact of Sec22b silencing on MHC I presentation of the C-terminal HF10 epitope. We differentiated bone marrow-derived DCs (BMDCs) from B6D2 F1 mice that express both K^b and L^d, the two MHC I molecules that present the SAG1-OVA-derived SL8 and the GRA6-derived HF10 peptides, respectively. As expected, lentivirus-based silencing of Sec22b in BMDCs led to a dramatic reduction in Sec22b protein level (Fig. 1A). Sec22b-silenced BMDCs were infected with increasing MOI of TgPru *Tomato SAG1-OVA*, a red fluorescent type II *T. gondii* that secretes SAG1-OVA and GRA6(II) in the PV *via* dense granules [28] (Fig. 1B and Table 1). We did not observe any adverse effect of Sec22b silencing on BMDC viability (Fig. 1C) or infection rate (Fig. 1D and Supporting Information Fig. 1). Using BTg01Z, a β-gal-inducible reporter $CD4^+$ T cell hybridoma that recognizes AS15, a *T. gondii* MHC class II epitope derived from TGME49_212300 [29], we also found no impact of Sec22b silencing on MHC II presentation (Fig. 1E). In line with our previous observations [13], Sec22b silencing reduced presentation of the SAG1-OVA-derived K^b-SL8 complex, as measured with the B3Z reporter hybridoma (Fig. 1F). However there was no change in presentation of the L^d-HF10 complex, as assessed with the CTgEZ.4 reporter hybridoma (Fig. 1G). These results indicate that in contrast to SAG1-OVA, GRA6 presentation does not rely on Sec22b-mediated host ER-PV connections.

Determination of GRA6 topology at the PV membrane and inversion of epitope orientation

In the PV, around half of GRA6 behaves as an integral transmembrane protein and the other half remains soluble [23, 27]. Since we previously showed that the soluble fraction of GRA6 is poorly presented by MHC I [27], we focused on the determinants that

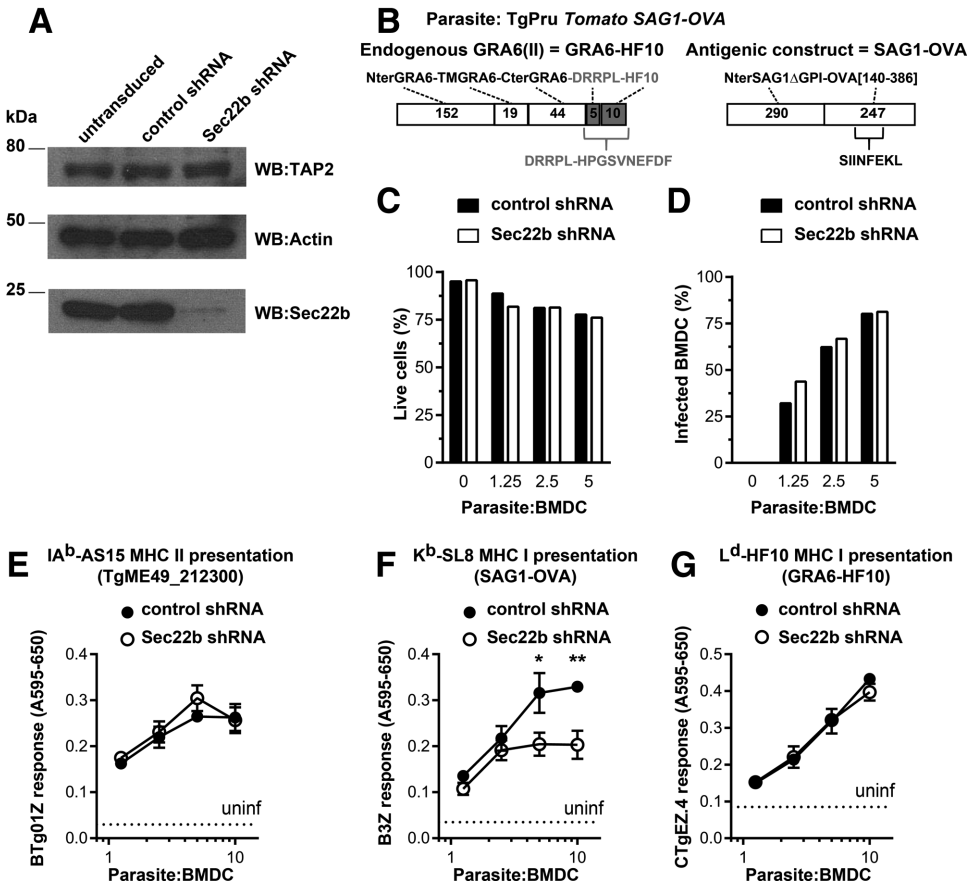

Figure 1. Sec22b is not required for presentation of the GRA6-derived HF10 epitope by infected dendritic cells. (A) Western blot analysis of Sec22b expression (lower panel) at day 9 of B6D2 F1 BMDC differentiation, following transduction with a non-target control shRNA or with an shRNA targeting Sec22b. TAP2 (upper panel) and actin (middle panel) are loading controls. (B) Schematic representation of the endogenous GRA6-HF10 (i.e. GRA6(II)) protein and the SAG1-OVA antigenic construct expressed by TgPru *Tomato SAG1-OVA*. Endogenous GRA6-HF10 comprises Nter GRA6(II) – TM GRA6(II) – Cter GRA6(II) domains, including the C-terminal HPGSVNEFDF (HF10) peptide flanked by the DRRPL sequence. Transgenic SAG1-OVA comprises the SAG1 (minus GPI) – OVA[140-386] domains, including the SIINFEKL peptide. Numbers represent the size of each domain in amino acids (aa). (C) Proportion of live (= viability dye-negative) cells at 8 h of infection with increasing MOI of TgPru *Tomato SAG1-OVA*. (D) Proportion of TgPru *Tomato SAG1-OVA*-infected BMDCs (i.e. Tomato$^+$ out of live CD11c$^+$ MHCI K^{b+} cells) measured 8 h post-infection. (E) IA^b-AS15 MHC class II presentation by the indicated BMDCs infected for 8 h with TgPru *Tomato SAG1-OVA*, assessed with the BTg01Z hybridoma. (F) K^b-SL8 MHC class I presentation by the indicated BMDCs infected for 8 h with TgPru *Tomato SAG1-OVA*, assessed with the B3Z hybridoma. (G) L^d-HF10 MHC class I presentation by the indicated BMDCs infected for 8 h with TgPru *Tomato SAG1-OVA*, assessed with the CTgEZ.4 hybridoma. (E–G) Data are shown as mean ± SD ($n = 3$). $^*p < 0.05$; $^{**}p < 0.005$, obtained with multiple nonparametric t tests without assuming consistent SD. Data depicted are representative of 2 (A, C, D, E) or 3 (F, G) experiments. Dotted lines show the hybridoma basal responses with uninfected BMDCs.

could regulate presentation of membrane-bound GRA6, including its orientation at the PV membrane. To determine GRA6 topology, we worked with type I TgRH parasites engineered to express type II GRA6, in which endogenous type I GRA6 (i.e. GRA6-HY10) and transgenic type II GRA6 (i.e. GRA6-HF10) can be simultaneously visualized. These parasites are referred to herein as TgRH *GRA6-HF10* (Fig. 2A and Table 1). We optimized a differential permeabilization assay that relies on the property of digitonin to selectively permeabilize the host cell plasma membrane and of saponin to permeabilize both the host cell plasma membrane and the PV

Table 1. List of parental and transgenic *T. gondii* used in this study

Short name	Complete description, with full genotype	Reference
TgPru *Tomato SAG1-OVA*	Pru.*tdTomato*$^{\text{prom tub}}$.*SAG1ΔGPI-OVA[140-386]*$^{\text{prom tub 3'utr dhfr}}$ +*BLE*	[55]
TgRH	RH.Δ*hxgprt*	[56]
TgRH *GRA6-HF10*	RH.Δ*hxgprt.GRA6(II)*$^{\text{prom GRA6(II) 3'utr GRA6(II)}}$ +*HXGPRT*	this study
TgRH *GRA5-HF10*	RH.Δ*hxgprt.GRA5(I)-DRRPL-HF10*$^{\text{prom GRA5(I) 3'utr GRA5(I)}}$ +*HXGPRT*	this study
TgCEP *GRA6(II)-HA*	CEP.Δ*hxgprt.GFP*$^{\text{prom GRA2}}$.*click beetle LUC*$^{\text{prom DHFR}}$.*GRA6(II)-HA*$^{\text{prom GRA1 3'UTR GRA2}}$+*HXGPRT*	[22]

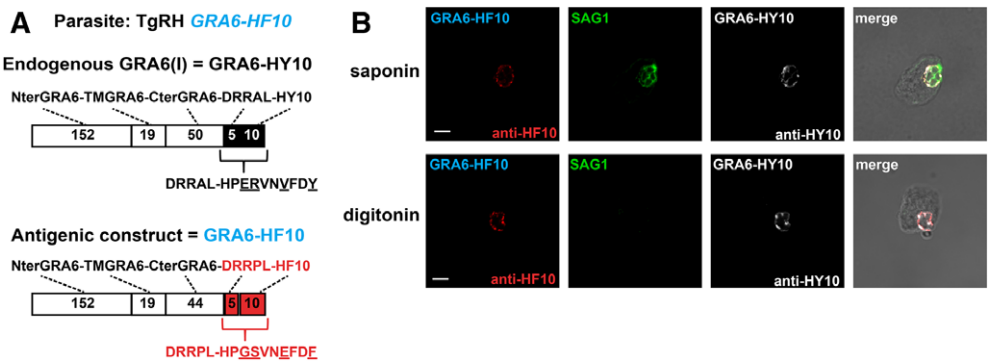

Figure 2. Type I and type II GRA6 are inserted at the PV membrane with the C-terminus facing the host cell cytosol. (A) Schematic representation of the endogenous and transgenic GRA6 proteins expressed by TgRH *GRA6-HF10*. Endogenous GRA6(I) comprises Nter GRA6(I) – TM GRA6(I) – Cter GRA6(I) domains, including the C-terminal HPERVNVFDY (HY10) peptide flanked by the DRRAL sequence. Transgenic GRA6-HF10 comprises Nter GRA6(II) – TM GRA6(II) – Cter GRA6(II) domains, including the C-terminal HPGSVNEFDF (HF10) peptide flanked by the DRRPL sequence. Numbers represent the size of each domain in aa. Underlined letters show polymorphisms of the C-terminal peptide between type I and type II GRA6. (B) Differential permeabilization assay with saponin (upper panel) to permeabilize both the host cell plasma membrane and the PV membrane and digitonin (lower panel) to only permeabilize the host cell plasma membrane. Immunofluorescence staining of BMMs infected for 20 h with TgRH *GRA6-HF10*. Red: GRA6-HF10 detected with anti-HF10. Green: SAG1. White: endogenous GRA6(I) detected with anti-HY10. Representative pictures from > 5 cells per condition, acquired with the same settings. Scale bar: 5 μm.

membrane. Applying this method in fibroblasts, GRA5 C-terminus was found to be present within the PV lumen [24]. We adjusted it for use in BM-derived macrophages (BMMs) and we validated by confocal microscopy that SAG1, an abundant protein decorating the parasite plasma membrane, was detected with saponin but not with digitonin (Fig. 2B). We then took advantage of non-cross-reactive rabbit antisera raised against the polymorphic C-terminus of type I GRA6-HY10 (HPERVNVFDY, HY10) and of type II GRA6-HF10 (HPGSVNEFDF, HF10) [27] (Supporting Information Fig. 2). Both HY10 and HF10 extremities were detected in saponin- and in digitonin-treated cells (Fig. 2B), indicating that regardless of the polymorphisms, the C-termini of type I and type II GRA6 are exposed to the host cytosol. Similar results were obtained with anti-HA antibodies used to detect an HA-tagged version of type II GRA6 expressed by type III TgCEP parasites (Supporting Information Fig. 3). To evaluate whether orientation of the HF10 epitope impacts MHC I presentation, we sought to invert this orientation and thus appended HF10 at the C-terminus of GRA5. Since flanking residues of a T cell epitope can strongly affect processing efficiency [30–32], we kept the 5 N-terminal flanking residues of HF10: DRRPL. TgRH parasites expressing GRA5-DRRPL-HF10 are referred to here as TgRH *GRA5-HF10* (Fig. 3A). Again, SAG1 was detected only after saponin permeabilization and endogenous GRA6(I) was visible both after saponin and digitonin treatments (Fig. 3B). This time however, the C-terminal HF10 peptide on the GRA5-HF10 antigenic construct was not visible after digitonin permeabilization (Fig. 3B), confirming that when fused to GRA5, HF10 faces the PV lumen. To document the topology of both antigenic constructs on a larger number of cells, we adapted the differential permeabilization assay for flow cytometry. We infected BMMs with two clones of each transfectant and labeled them separately with the antibodies. As depicted on Fig. 3C and in accordance with the above microscopical observations: (i) the C-termini of GRA6(I) and GRA6-HF10 were visible after both saponin and digitonin treatments (ii) SAG1 and GRA5-HF10 C-terminus were very poorly detected after digitonin permeabilization. Quantification of the ratio of percent marker-positive BMMs in digitonin over percent marker-positive BMMs in saponin confirmed these observations (Fig. 3D). When HF10 was cytosol-exposed (i.e. GRA6-HF10), the digitonin:saponin ratio for HF10 was similar to the ratio for endogenous HY10. When HF10 was lumen-exposed (i.e. GRA5-HF10), the ratio for HF10 was lower and similar to that of SAG1. Altogether these results demonstrate that the C-terminus of GRA6-HF10 protrudes into the host cytosol and the C-terminus of GRA5-HF10 faces the PV lumen. They provide useful tools (Fig. 3E) to study the influence of topology on MHC I presentation.

Exposure of the epitope to host cytosol favors efficient MHC I presentation

To this aim, we infected BMMs with 2 clones of each transfectant and we measured presentation of HF10 with the CTgEZ.4 hybridomas. L^d-HF10 presentation by BMMs infected with TgRH *GRA5-HF10* was strongly reduced as compared to BMMs infected with TgRH *GRA6-HF10* (Fig. 4A). This difference could not be attributed to impaired infectivity of TgRH *GRA5-HF10* (Fig. 4B) or to defective expression of the GRA5-HF10 antigenic construct (Fig. 4C). Indeed quantification of the antigen expression levels in extracellular tachyzoites using the anti-HF10 antibody, revealed that GRA5-HF10 was at least as abundant as GRA6-HF10 (Fig. 4D). Previous studies reported that GRA5 and GRA6 may directly modulate the function of innate immune cells [33, 34], which could affect the T cell stimulation ability of infected BMMs independently of the intrinsic antigenicity of GRA5-HF10 and GRA6-HF10. To evaluate this potential confounding factor, we measured presentation of the exogenously pulsed peptide SM9

thanks to BDSM9Z reporter hybridomas [27]. L^d-SM9 presentation by infected BMMs was similar regardless of the constructs (Fig. 4E), ruling out that the antigenic constructs influence the general ability of the macrophages to present antigens. We next analyzed HF10 presentation by DCs, the most competent cell type for priming a T-cell response, infected by the TgRH transfectants which had similar antigenic construct level (Fig. 4C and D). Again, there was a dramatic decrease in L^d-HF10 presentation by TgRH *GRA5-HF10*-infected BMDCs (Supporting Information Fig. 4A) despite a similar infection rate (Supporting Information Fig. 4B) and an identical ability of the infected BMDCs to present exogenous SM9 (Supporting Information Fig. 4C). In summary, these data show that MHC I presentation of the PV transmembrane GRA6 antigen by infected macrophages and DCs is most efficient when the antigenic peptide faces the host cytosol. As Sec22b was important for presentation of the luminal soluble SAG1-OVA antigen (see Fig. 1), we finally addressed whether Sec22b was also necessary for presentation of the luminal-pointing HF10 peptide in the GRA5-HF10 context. To this end, we transduced the RAW309 macrophage cell line ($H2^{bxd}$) with Sec22b-targeting *versus* non-target control shRNA lentiviruses, infected them with TgRH *GRA6-HF10* and TgRH *GRA5-HF10*, and assessed HF10 presentation with the CTgEZ.4 hybridomas. We chose to work with TgRH *GRA5-HF10* clone 2 since it led to a measurable T cell response, in contrast to clone 1 (see Fig. 4A). As shown on Supporting Information Fig. 5A, Sec22b protein expression was reduced in the Sec22b shRNA-transduced RAW. Sec22b was not required for HF10 presentation when derived from GRA6-HF10 (i.e. cytosol-pointing), confirming that transgenic GRA6-HF10 in the TgRH strain behaves similarly as endogenous GRA6(II) in the TgPru strain (Supporting Information Fig. 5B). Importantly, as shown on Supporting Information Fig. 5C, MHC I presentation of luminal HF10 was not reduced in Sec22b-silenced RAW, suggesting that presentation of HF10 in this context does not need recruitment of the ERGIC-associated Sec22b-dependent host machinery.

Discussion

In this work, we provide substantial new insights into the pathway used for processing of the immunodominant and protective *T. gondii* GRA6 antigen. First, by evaluating the impact of Sec22b silencing on GRA6 presentation, we found no evidence for the implication of the ER-PV fusion pathway contrary to what was known, and further confirmed here, for the soluble SAG1-OVA antigen [12, 13]. ER-PV fusion is an intriguing process, initially described with regular phagosomes [14, 35], which constitutes an escape route to the cytosol for luminal *T. gondii* antigens. Mediated by the ER-Golgi Intermediate Compartment (ERGIC) Sec22b SNARE protein, the fusion of ER-derived vesicles onto the PV is thought to recruit ERAD components at the PV membrane, in particular the Sec61 translocon protein [12]. ERAD is a quality-control process aimed to remove misfolded proteins from the ER. ERAD is performed by a multimeric assembly including Sec61, receptors (e.g. Derlin 1), lectins (e.g. OS9) and E3 ubiquitin ligases (e.g. Hrd1, TRC8, TMEM) (reviewed in [36, 37]), which retro-translocates substrates to the cytosol and marks them for proteasomal degradation. Why in contrast to SAG1-OVA, is presentation of GRA6 not affected by Sec22b silencing? Of note, GRA6 behaves partly as a transmembrane protein after release in the PV and only the membrane-bound GRA6 is efficiently presented by MHC I [27]. While integral membrane proteins can also be ERAD substrates, their proteasomal degradation typically requires prior dislocation from the membrane. A major driving force for the dislocation reaction is typically provided by the p97/valosin-containing protein AAA ATPase [38]. Hence one possibility is that the machinery imported via Sec22b onto the PV membrane lacks this important factor. Another possibility is that import of the 'dislocase' machinery may occur independently from Sec22b and independently from ER-PV fusion. Studying whether p97 and membrane extraction are involved in GRA6 processing are exciting further prospects that should help disentangle these hypotheses.

Remarkably, several proteins that insert within the limiting membrane of the *Chlamydia trachomatis* intracellular compartment (also named inclusion) are major $CD8^+$ T-cell antigens [39–41]. Although the *Chlamydia* inclusion does not appear to fuse with the ER, very close contacts are established between both compartments (reviewed in [42]). Whether Sec22b, ERAD components and/or topology of the *Chlamydia* antigens contribute to their MHC I presentation is unknown and deserves further research.

Of note, in an inflammatory context, additional processes have been shown to play a role in MHC I processing. In IFNγ-stimulated cells, PV recruitment of Immunity-Related GTPases, such as Irgm3 [43], as well as ubiquitin-binding proteins, such as p62/Sqstm1 [44], indeed contribute to MHC I presentation of vacuolar antigens (e.g. SAG1-OVA). In the future, it would be interesting to study the roles of these IFNγ-triggered cell-autonomous effectors in HF10 presentation using the two membrane-anchored antigens that have inverse topologies.

Which protease(s) could be involved in degradation of the PV membrane-bound GRA6? Based on (i) the involvement of 'cytosolic' players of the MHC I pathway in GRA6 presentation, e.g. proteasome, TAP and the ER-associated aminopeptidase (ERAAP) [16], (ii) the importance of the epitope C-terminal location [22] and (iii) the exposure of GRA6 C-terminus to the host cytosol (this study), we favor a model in which a yet unknown protease would clip and liberate the HF10-containing C-terminal domain of GRA6 for final processing by the 'cytosolic' MHC I pathway. This protease may be cytosolic or membrane-bound. Several intramembrane proteases located in various subcellular compartments indeed control the membrane proteome. Those include aspartate proteases such as the signal peptide peptidase (SPP) and SPP-like (SPPL), and serine proteases of the rhomboid family [45]. Interestingly, SPP was reported to liberate an epitope located in the membrane-embedded C-terminus of an ER protein [46, 47], showing that intramembrane proteolysis contributes to MHC I presentation of endogenous membrane proteins. However to our knowledge, the role of intramembrane proteolysis has never been examined in

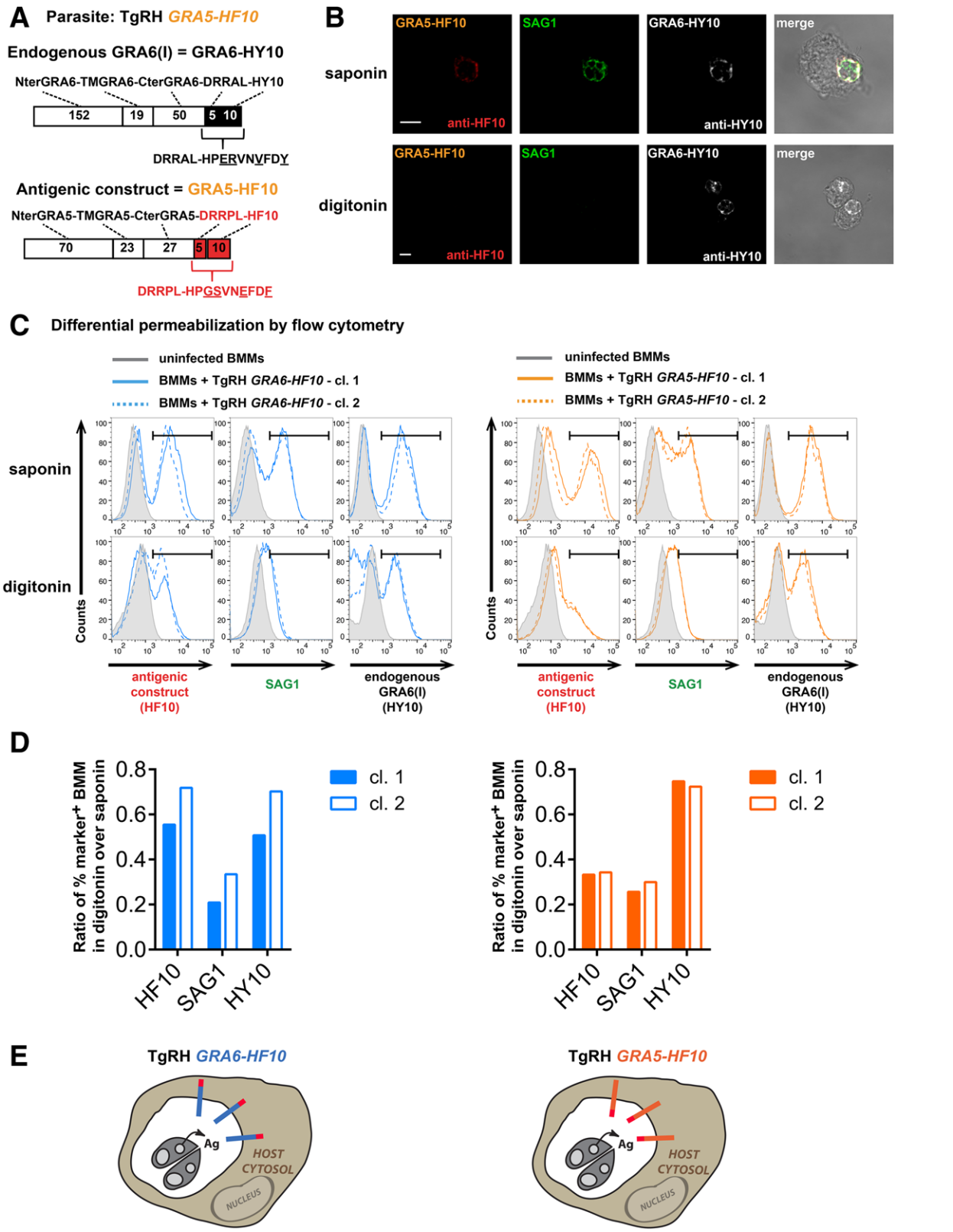

Figure 3. GRA5-HF10 is inserted at the PV membrane with the C-terminus facing the PV lumen. (A) Schematic representation of the endogenous GRA6(I) and transgenic GRA5-HF10 proteins expressed by TgRH *GRA5-HF10*. Endogenous GRA6(I) comprises Nter GRA6(I) – TM GRA6(I) – Cter GRA6(I) domains, including the C-terminal DRRAL-HY10 sequence. Transgenic GRA5-HF10 comprises Nter GRA5 – TM GRA5 – Cter GRA5 domains, appended with the last 15 aa of GRA6-HF10: DRRPL-HPGSVNEFDF (red). Numbers represent the size of each domain in aa. Underlined letters show polymorphisms within the C-terminal decameric peptide between type I and type II GRA6. (B) Differential permeabilization assay with saponin

cross-presentation. In addition to fusion with ERGIC-derived vesicles, the *T. gondii* PV is known to intercept the host Golgi to scavenge sphingolipids [48] and to interact with Rab22a-containing recycling endosomes [49]. In this context, it is tempting to speculate that intramembrane proteases present in the Golgi (e.g. RHBDL1 [50]) or the endosomes (e.g. SPPL2b [51]) may gain access to the PV membrane and hydrolyze peptide bonds within GRA6 TM domain. If such a scenario applies, the lower MHC I presentation of HF10 in the context of GRA5 may also be linked to substrate selectivity for GRA6 TM over GRA5 TM domain. At last it is interesting to note that this scenario could have implications beyond antigen presentation as type I GRA6 C-terminus has been reported to stimulate NFAT4 activity [34]. The 'clipping' peptidase could thus also modulate innate signals.

From a vaccine point of view, our findings should be useful to harness *T. gondii* more effectively as a vaccine vector. Perhaps like oncolytic viruses which have been approved as anti-tumor therapeutic agents [52], *T. gondii* could become an additional weapon in the anti-cancer arsenal. Pioneering studies have shown that an attenuated strain of *T. gondii* can promote antitumor immunity due to a strong adjuvant effect [53, 54]. To fully exploit the potential of *T. gondii* not only as an adjuvant but also as an antigen-carrying T cell-boosting vehicle, it will now be essential to take the biochemical properties of the tumor antigen(s) (e.g. PV membrane association, topology) into consideration in order to find the most immunogenic context.

In summary, our results underline the diversity and complexity of the pathways that lead to $CD8^+$ T-cell recognition of *T. gondii* peptide fragments. Mechanisms may differ depending on the antigen biochemical properties (e.g. soluble vs membrane-bound and cytosol- vs lumen-oriented). This knowledge will be invaluable to design vaccine strategies against *T. gondii* and to optimize the immune stimulatory potential of that parasite against cancer.

Materials and methods

Mice, parasites, and antibodies

C57BL/6JxDBA/2 F1 (B6D2) mice were purchased from Janvier (France) and housed under specific pathogen-free conditions. Mice were first anesthetized by isoflurane inhalation and euthanized by cervical dislocation. No protocol involving pain was used in this study.

T. gondii strains are listed in Table 1. Parasites were maintained by serial passages on confluent monolayers of human foreskin fibroblasts (HFF, ATCC SCRC-1041).

Primary antibodies for Western blot, flow cytometry and immunofluorescence were rabbit anti-TAP2 (H-210, Santa Cruz), mouse anti-actin (Sigma), rabbit anti-Sec22b (Synaptic Systems), rabbit anti-HA (Sigma), purified rabbit anti-HF10 and anti-HY10 sera (custom-made, Biotem, Grenoble), mouse anti-SAG1 (TP3, Santa Cruz) and mouse anti-GRA1 (TG17.43, Biotem).

Plasmid constructs and parasite transfection

Plasmids were constructed either by traditional ligation or by fusion of a PCR amplicon into an opened vector using the In-Fusion HD Cloning kit (Clontech). The plasmid containing GRA6(II) coding sequence flanked by the endogenous GRA6(II) 5' and 3' UTR plus the HXGPRT selectable marker, used to generate TgRH *GRA6-HF10* parasites, was described previously [22]. The plasmid encoding GRA5-HF10 flanked by the endogenous GRA5 5' and 3' UTR, used to generate TgRH *GRA5-HF10* parasites, was obtained by PCR amplification of GRA5 from TgPru genomic DNA using the following forward and reverse primers: 74F: 5′-ATGGCGTCTCCCGGGAACAAAATGGCGTCTGTAAAAC and 204R: 5′-GCTTCTATCAAGATCTTTAAAAATCAAACTCATTCACACTTCC CGGGTGCAACGGGCGCCTGTCCTCTTCCTCGGCAACTTCTTC, introducing the DRRPL-HF10 sequence upstream of the GRA5 STOP codon as well as floating extremities of 15 bp overlapping with the vector. The resulting GRA5-HF10 PCR amplicon was fusion-cloned into the XmaI-BglII-opened pKS+ 5'UTR GRA5 / 3'UTR GRA5 vector [27].

Parasite transfections were performed as previously described [27]. In brief, 2×10^7 freshly egressed tachyzoites were electroporated with 50 μg of linearized plasmid containing the HXGPRT selectable marker, or 50 μg of linearized plasmid without selectable marker plus 5 μg of pmini/HXGPRT. Tachyzoites were seeded in $4 \times 25\text{-cm}^2$ flasks of HFF and selection was achieved with xanthine and mycophenolic acid. Tachyzoites from resistant bulks were cloned by limiting dilution in 96-well plates.

Western blot

Tachyzoites were released from infected HFF with a 23-G needle, lyzed in 1× Laemmli buffer 1× and heated for 5 min

(upper panel) to permeabilize both the host cell plasma membrane and the PV membrane or digitonin (lower panel) to selectively permeabilize the host cell plasma membrane. Immunofluorescence staining of BMMs infected for 20 h with TgRH *GRA5-HF10*. Red: GRA5-HF10, detected with anti-HF10. Green: SAG1. White: endogenous GRA6(I) detected with anti-HY10. Representative pictures from > 5 cells per condition, acquired with the same settings. Scale bar: 5 μm. (C) Flow cytometry analysis of the differentially permeabilized cells. BMMs infected for 20 h with two clones of TgRH *GRA6-HF10* (blue, left panels) and two clones of TgRH *GRA5-HF10* (orange, right panels) were permeabilized with saponin (upper panels) or digitonin (lower panels) and single-labeled with the indicated antibodies. Grey-shaded histograms represent uninfected BMMs labeled with the same primary and secondary antibodies. (D) Bar graphs show the ratio of percent marker-positive BMMs in digitonin over percent marker-positive BMMs in saponin for TgRH *GRA6-HF10* (blue) and TgRH *GRA5-HF10* (orange). Plots in (C, D) are representative of two independent experiments. (E) Schematic representation of antigenic construct opposite orientations at the PV membrane in infected cells. The HF10 epitope is symbolized in red.

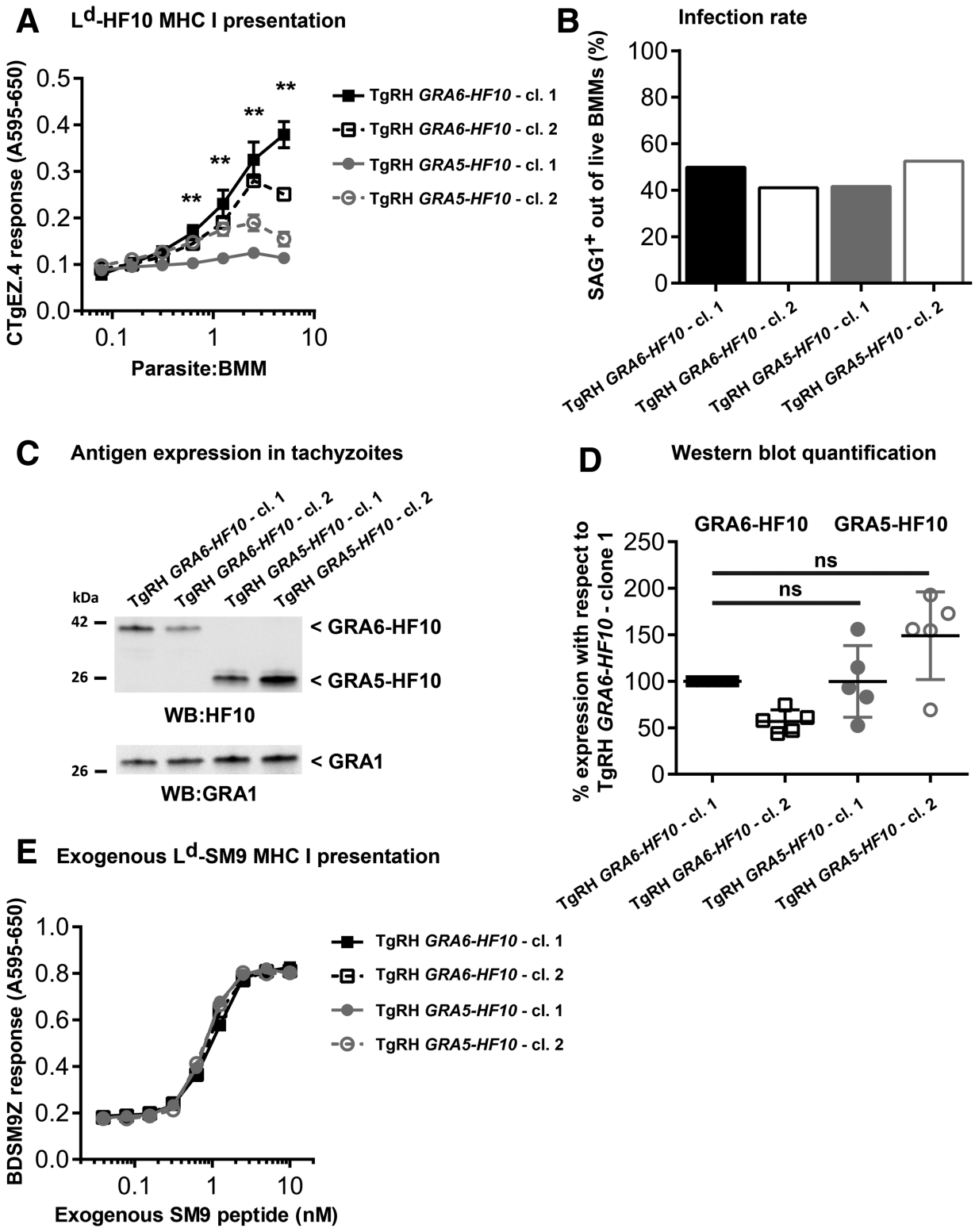

Figure 4. Orientation of the epitope toward the host cytosol favors MHC class I presentation in infected macrophages. (A) L^d-HF10 presentation by BMMs infected for 20 h with the indicated parasites, assessed with the CTgEZ.4 hybridoma. Asterisks show the statistically significant differences between TgRH *GRA6-HF10* – clone 1 and TgRH *GRA5-HF10* – clone 1 at the different MOI (triplicates). Data are shown as mean ± SD ($n = 3$). $^{**}p < 0.005$, obtained with multiple non-parametric t tests without assuming consistent SD. (B) Proportion of *T. gondii*-infected ($SAG1^+$) cells out of live BMMs, measured by intracellular flow cytometry at 20 h post-infection. (C) Western blot analysis showing the expression level of GRA6-HF10 and GRA5-HF10 in extracellular tachyzoites, revealed with rabbit anti-HF10 antiserum (upper panel) and an anti-GRA1 mAb as a loading control

at 60°C in reducing conditions. The equivalent of 10^6 parasites was loaded, separated by electrophoresis and transferred to nitrocellulose membranes. Immunologic detection was performed using horseradish peroxidase-conjugated antibodies (Promega) and quantified using a ChemiDoc XRS+ system (Bio-Rad).

BMM and BMDC differentiation, lentiviral transduction and antigen presentation assays

These experiments were performed as previously described [27]. In brief, bone marrow cells were retrieved from femurs and tibias. Macrophages were differentiated for 7 days in Petri dishes with RPMI (Invitrogen) supplemented with 20% (vol/vol) fetal calf serum (FCS, Hyclone) and 10% (vol/vol) colony-stimulating factor (CSF)–containing culture supernatant (~ 95% $CD11b^+$). DCs were differentiated for 6–8 days with 10% (vol/vol) of granulocyte-macrophage colony-stimulating factor (GM-CSF)-containing culture supernatant in complete RPMI medium (~ 70% $CD11c^+$). Lentiviral transduction of BMDCs with shRNA to silence Sec22b was achieved as previously reported [13]. In summary, BMDCs were transduced by 'spinfection' from day 4 to day 6 in the presence of lentiviral particles plus 8 μg / ml of polybrene, and selected by puromycin between day 6 and day 9. The following shRNA were used: shRNA Sec22b (clone ID TRC N0000115089): 5'-CCGGCCCTATTCCTTCATCGAGTTTCTCGAGAAACTCGAGAA GGAATAGGGTTTTG and control (non-target) shRNA: 5'-CCGGCAACAAGATGAAGAGCACCAACTCGAGTTGGTGCTCTTCA TCTTGTTGTTTTT, coding for a sequence that does not match any mouse or human mRNA.

For antigen presentation, BMMs and BMDCs were seeded into flat-bottom 96-well plates and infected for 8 h or 24 h with serially diluted tachyzoites. The proportion of infected cells (i.e. $Tomato^+$ or $SAG1^+$) was controlled by flow cytometry, following fixation and saponin permeabilization in the case of SAG1 staining. Presentation of HF10 by L^d, SM9 by L^d and SL8 by K^b was assessed after 16 h of incubation with the CTgEZ.4 [16], BDSM9Z [22] and B3Z [13] reporter hybridomas, respectively. Production of β-galactosidase by the hybridomas was quantified using the chromogenic substrate chlorophenol red-β-D-galactopyranoside (CPRG, Roche). Absorbance was read at 595 nm with a reference at 655 nm.

Differential permeabilization

10^7 BMMs were plated in Petri dishes and infected at MOI 1:1. After 20 h, BMMs were detached with cold PBS-EDTA 5 mM and transferred into 15 mL centrifuge tubes. The followings steps were performed on ice, using cold media and refrigerated centrifuges. Cells were washed with PBS, incubated with the viability dye eFluor 450 (eBioscience), fixed for 15 min with PFA 3% and quenched with PBS glycine 0.2 M. Permeabilization was achieved either with PBS-BSA 0.2%-Saponin 0,05% or with PBS-digitonin 0.0005% for 5 min. Cells were then washed with 10 mL of cold PBS and suspended in PBS-BSA 0.2%-Saponin 0,05% or PBS-BSA 3% for the cells treated with digitonin. For immunofluorescence, cells were stained for 30 min on ice with biotinylated rabbit anti-HF10 antibodies, AF647-coupled rabbit anti-HY10 antibodies and mouse anti-SAG1 antibody, followed by incubation with streptavidin-AF488 (Thermo fisher) and anti-mouse AF555 (Life Science). Cells were then centrifuged and suspended in 10 μL of Mowiol for mounting and visualization with a Zeiss LSM 710 confocal microscope. For flow cytometry, after permeabilization, cells were incubated with FcR Block (eBioscience), labeled individually with primary antibodies (purified rabbit anti HY10, purified rabbit anti HF10 or mouse anti SAG-1) followed by an AF488-coupled secondary antibody (Life Technologies). PBS-BSA 0.2%-Saponin 0,05% was used for incubations of the saponin-permeabilized samples. Cells were acquired with a MACSQuant10 flow cytometer (Miltenyi Biotech).

Statistical analyses

The Prism software (GraphPad) was used for statistical analyses. Multiple non-parametric t tests without assuming consistent s.d. were used for antigen presentation assays and Wilcoxon signed-rank tests for Western blot quantifications, where the median for each TgRH *GRA5-HF10* clone was compared to 100, the value assigned to TgRH *GRA6-HF10* – clone 1. $^{**}p$ value < 0.005; $^{*}p$ value < 0.05; ns: p value > 0.05.

Acknowledgements: The CPTP flow cytometry and imaging core facilities, the Blanchard team for help and discussions; C. Bonnart and M.-F. Cesbron-Delauw for critical reading of the manuscript. Conceived and designed the experiments: CB NAG IC SB JL NB. Performed the experiments: CB NAG IC SB JL EBVV JSR. Analyzed the data: CB NAG IC SB JL NB JSR. Wrote the paper: NB with help of coauthors. This work was supported by 'Institut National de la Santé et de la Recherche Médicale' and the 'Fondation Bettencourt-Schueller' (Avenir Grant to NB), 'Agence Nationale de la Recherche' (ANR-11-BSV3-01002 to NB), 'Région Midi-Pyrénées' (NB), Human Frontier Science Program Organization

(lower panel). Blots are representative of five independent experiments. (D) Quantification of the Western blot signals by densitometry in lysates from five independent experiments. Expression of the HF10-containing antigen was normalized with GRA1 for each clone. Data are shown as mean ± SD of the percentage of expression of the HF10-containing antigen, with respect to TgRH *GRA6-HF10* – clone 1. (E) Exogenous MHC I presentation of synthetic SM9 peptide pulsed on BMMs that were previously infected with the indicated parasites for 20 h, assessed with the BDSM9Z T cell hybridoma. (A, B, E) Data shown are representative of two independent experiments.

(CDA00047/2011 to NB), PIA PARAFRAP Consortium (ANR-11-LABX0024 to NB), PIA ANINFIMIP equipment (ANR-11-EQPX-0003 to NB), 'Ministère de l'Education Nationale, de la Recherche et de la Technologie' (CB), 'Fondation pour la Recherche Médicale' (JL), ECOS-Sud (action A13S01 to NB and IC).

Conflict of interest: The authors declare no commercial or financial conflict of interest.

References

1 **Montoya, J. G. and Liesenfeld, O.**, Toxoplasmosis. *Lancet* 2004. **363:** 1965–1976.

2 **Demar, M., Hommel, D., Djossou, F., Peneau, C., Boukhari, R., Louvel, D., Bourbigot, A. M. et al.**, Acute toxoplasmoses in immunocompetent patients hospitalized in an intensive care unit in French Guiana. *Clin. Microbiol. Infect.* 2012. **18:** E221–E231.

3 **Blanchard, N. and Shastri, N.**, Cross-presentation of peptides from intracellular pathogens by MHC class I molecules. *Ann. N. Y. Acad. Sci.* 2010. **1183:** 237–250.

4 **Suzuki, Y. and Remington, J. S.**, Dual regulation of resistance against Toxoplasma gondii infection by Lyt-2+ and Lyt-1+, L3T4+ T cells in mice. *J. Immunol.* 1988. **140:** 3943–3946.

5 **Brown, C. R., Hunter, C. A., Estes, R. G., Beckmann, E., Forman, J., David, C., Remington, J. S. et al.**, Definitive identification of a gene that confers resistance against Toxoplasma cyst burden and encephalitis. *Immunology* 1995. **85:** 419–428.

6 **Khan, I. A., Ely, K. H. and Kasper, L. H.**, Antigen-specific CD8+ T cell clone protects against acute Toxoplasma gondii infection in mice. *J. Immunol.* 1994. **152:** 1856–1860.

7 **Kwok, L. Y., Lutjen, S., Soltek, S., Soldati, D., Busch, D., Deckert, M. and Schluter, D.**, The induction and kinetics of antigen-specific CD8 T cells are defined by the stage specificity and compartmentalization of the antigen in murine toxoplasmosis. *J. Immunol.* 2003. **170:** 1949–1957.

8 **Gregg, B., Dzierszinski, F., Tait, E., Jordan, K. A., Hunter, C. A. and Roos, D. S.**, Subcellular antigen location influences T-cell activation during acute infection with toxoplasma gondii. *PloS One* 2011. **6:** e22936.

9 **Dupont, C. D., Christian, D. A., Selleck, E. M., Pepper, M., Leney-Greene, M., Harms Pritchard, G., Koshy, A. A. et al.**, Parasite fate and involvement of infected cells in the induction of CD4+ and CD8+ T cell responses to toxoplasma gondii. *PLoS Pathog.* 2014. **10:** e1004047.

10 **Bertholet, S., Goldszmid, R., Morrot, A., Debrabant, A., Afrin, F., Collazo-Custodio, C., Houde, M. et al.**, Leishmania antigens are presented to CD8+ T cells by a transporter associated with antigen processing-independent pathway in vitro and in vivo. *J. Immunol.* 2006. **177:** 3525–3533.

11 **Gubbels, M. J., Striepen, B., Shastri, N., Turkoz, M. and Robey, E. A.**, Class I major histocompatibility complex presentation of antigens that escape from the parasitophorous vacuole of Toxoplasma gondii. *Infect. Immun.* 2005. **73:** 703–711.

12 **Goldszmid, R. S., Coppens, I., Lev, A., Caspar, P., Mellman, I. and Sher, A.**, Host ER-parasitophorous vacuole interaction provides a route of entry for antigen cross-presentation in Toxoplasma gondii-infected dendritic cells. *J. Exp. Med.* 2009. **206:** 399–410.

13 **Cebrian, I., Visentin, G., Blanchard, N., Jouve, M., Bobard, A., Moita, C., Enninga, J. et al.**, Sec22b regulates phagosomal maturation and antigen crosspresentation by dendritic cells. *Cell* 2011. **147:** 1355–1368.

14 **Guermonprez, P., Saveanu, L., Kleijmeer, M., Davoust, J., Van Endert, P. and Amigorena, S.**, ER-phagosome fusion defines an MHC class I cross-presentation compartment in dendritic cells. *Nature* 2003. **425:** 397–402.

15 **Alloatti, A., Kotsias, F., Magalhaes, J. G. and Amigorena, S.**, Dendritic cell maturation and cross-presentation: timing matters! *Immunol. Rev.* 2016. **272:** 97–108.

16 **Blanchard, N., Gonzalez, F., Schaeffer, M., Joncker, N. T., Cheng, T., Shastri, A. J., Robey, E. A. et al.**, Immunodominant, protective response to the parasite Toxoplasma gondii requires antigen processing in the endoplasmic reticulum. *Nat. Immunol.* 2008. **9:** 937–944.

17 **Frickel, E. M., Sahoo, N., Hopp, J., Gubbels, M. J., Craver, M. P., Knoll, L. J., Ploegh, H. L. et al.**, Parasite stage-specific recognition of endogenous Toxoplasma gondii-derived CD8+ T cell epitopes. *J. Infect. Dis.* 2008. **198:** 1625–1633.

18 **Wilson, D. C., Grotenbreg, G. M., Liu, K., Zhao, Y., Frickel, E. M., Gubbels, M. J., Ploegh, H. L. et al.**, Differential regulation of effector- and central-memory responses to Toxoplasma gondii Infection by IL-12 revealed by tracking of Tgd057-specific CD8+ T cells. *PLoS Pathog.* 2010. **6:**e1000815.

19 **Grover, H. S., Chu, H. H., Kelly, F. D., Yang, S. J., Reese, M. L., Blanchard, N., Gonzalez, F. et al.**, Impact of regulated secretion on antiparasitic CD8 T cell responses. *Cell Rep.* 2014. **7:** 1716–1728.

20 **Chu, H. H., Chan, S. W., Gosling, J. P., Blanchard, N., Tsitsiklis, A., Lythe, G., Shastri, N. et al.**, Continuous effector CD8(+) T cell production in a controlled persistent infection is sustained by a proliferative intermediate population. *Immunity* 2016. **45:** 159–171.

21 **Sanecka, A., Yoshida, N., Dougan, S. K., Jackson, J., Shastri, N., Ploegh, H., Blanchard, N. et al.**, Transnuclear CD8 T cells specific for the immunodominant epitope Gra6 lower acute-phase Toxoplasma gondii burden. *Immunology* 2016.

22 **Feliu, V., Vasseur, V., Grover, H. S., Chu, H. H., Brown, M. J., Wang, J., Boyle, J. P. et al.**, Location of the CD8 T cell epitope within the antigenic precursor determines immunogenicity and protection against the toxoplasma gondii parasite. *PLoS Pathog.* 2013. **9:** e1003449.

23 **Labruyere, E., Lingnau, M., Mercier, C. and Sibley, L. D.**, Differential membrane targeting of the secretory proteins GRA4 and GRA6 within the parasitophorous vacuole formed by Toxoplasma gondii. *Mol. Biochem. Parasitol.* 1999. **102:** 311–324.

24 **Gendrin, C., Mercier, C., Braun, L., Musset, K., Dubremetz, J. F. and Cesbron-Delauw, M. F.**, Toxoplasma gondii uses unusual sorting mechanisms to deliver transmembrane proteins into the host-cell vacuole. *Traffic* 2008. **9:** 1665–1680.

25 **Cesbron-Delauw, M. F., Gendrin, C., Travier, L., Ruffiot, P. and Mercier, C.**, Apicomplexa in mammalian cells: trafficking to the parasitophorous vacuole. *Traffic* 2008. **9:** 657–664.

26 **Mercier, C., Dubremetz, J. F., Rauscher, B., Lecordier, L., Sibley, L. D. and Cesbron-Delauw, M. F.**, Biogenesis of nanotubular network in Toxoplasma parasitophorous vacuole induced by parasite proteins. *Mol. Biol. Cell* 2002. **13:** 2397–2409.

27 **Lopez, J., Bittame, A., Massera, C., Vasseur, V., Effantin, G., Valat, A., Buaillon, C. et al.**, Intravacuolar membranes regulate CD8 T cell recognition of membrane-bound toxoplasma gondii protective antigen. *Cell Rep.* 2015.

28 **Chtanova, T., Han, S. J., Schaeffer, M., van Dooren, G. G., Herzmark, P., Striepen, B. and Robey, E. A.**, Dynamics of T cell, antigen-presenting cell, and pathogen interactions during recall responses in the lymph node. *Immunity* 2009. **31:** 342–355.

29 **Grover, H. S., Blanchard, N., Gonzalez, F., Chan, S., Robey, E. A. and Shastri, N.**, The Toxoplasma gondii peptide AS15 elicits CD4 T cells that can control parasite burden. *Infect. Immun.* 2012. **80:** 3279–3288.

30 **Le Gall, S., Stamegna, P. and Walker, B. D.**, Portable flanking sequences modulate CTL epitope processing. *J. Clin. Invest.* 2007. **117:** 3563–3575.

31 **Martinez, A. N., Tenzer, S. and Schild, H.**, T-cell epitope processing (the epitope flanking regions matter). *Methods Mol. Biol.* 2009. **524:** 407–415.

32 **Tenzer, S., Wee, E., Burgevin, A., Stewart-Jones, G., Friis, L., Lamberth, K., Chang, C. H. et al.**, Antigen processing influences HIV-specific cytotoxic T lymphocyte immunodominance. *Nat. Immunol.* 2009. **10:** 636–646.

33 **Persat, F., Mercier, C., Ficheux, D., Colomb, E., Trouillet, S., Bendridi, N., Musset, K. et al.**, A synthetic peptide derived from the parasite Toxoplasma gondii triggers human dendritic cells' migration. *J. Leukoc. Biol.* 2012. **92:** 1241–1250.

34 **Ma, J. S., Sasai, M., Ohshima, J., Lee, Y., Bando, H., Takeda, K. and Yamamoto, M.**, Selective and strain-specific NFAT4 activation by the Toxoplasma gondii polymorphic dense granule protein GRA6. *J. Exp. Med.* 2014. **211:** 2013–2032.

35 **Gagnon, E., Duclos, S., Rondeau, C., Chevet, E., Cameron, P. H., Steele-Mortimer, O., Paiement, J. et al.**, Endoplasmic reticulum-mediated phagocytosis is a mechanism of entry into macrophages. *Cell* 2002. **110:** 119–131.

36 **Smith, M. H., Ploegh, H. L. and Weissman, J. S.**, Road to ruin: targeting proteins for degradation in the endoplasmic reticulum. *Science* 2011. **334:** 1086–1090.

37 **Merulla, J., Fasana, E., Solda, T. and Molinari, M.**, Specificity and regulation of the endoplasmic reticulum-associated degradation machinery. *Traffic* 2013. **14:** 767–777.

38 **Carlson, E. J., Pitonzo, D. and Skach, W. R.**, p97 functions as an auxiliary factor to facilitate TM domain extraction during CFTR ER-associated degradation. *EMBO J.* 2006. **25:** 4557–4566.

39 **Fling, S. P., Sutherland, R. A., Steele, L. N., Hess, B., D'Orazio, S. E., Maisonneuve, J., Lampe, M. F. et al.**, CD8+ T cells recognize an inclusion membrane-associated protein from the vacuolar pathogen Chlamydia trachomatis. *Proc. Natl. Acad. Sci. USA* 2001. **98:** 1160–1165.

40 **Starnbach, M. N., Loomis, W. P., Ovendale, P., Regan, D., Hess, B., Alderson, M. R. and Fling, S. P.**, An inclusion membrane protein from Chlamydia trachomatis enters the MHC class I pathway and stimulates a CD8+ T cell response. *J. Immunol.* 2003. **171:** 4742–4749.

41 **Gervassi, A. L., Grabstein, K. H., Probst, P., Hess, B., Alderson, M. R. and Fling, S. P.**, Human CD8+ T cells recognize the 60-kDa cysteine-rich outer membrane protein from Chlamydia trachomatis. *J. Immunol.* 2004. **173:** 6905–6913.

42 **Derre, I.**, Chlamydiae interaction with the endoplasmic reticulum: contact, function and consequences. *Cell Microbiol.* 2015. **17:** 959–966.

43 **Dzierszinski, F., Pepper, M., Stumhofer, J. S., LaRosa, D. F., Wilson, E. H., Turka, L. A., Halonen, S. K. et al.**, Presentation of Toxoplasma gondii antigens via the endogenous major histocompatibility complex class I pathway in nonprofessional and professional antigen-presenting cells. *Infect. Immun.* 2007. **75:** 5200–5209.

44 **Lee, Y., Sasai, M., Ma, J. S., Sakaguchi, N., Ohshima, J., Bando, H., Saitoh, T. et al.**, p62 Plays a Specific Role in Interferon-gamma-Induced Presentation of a Toxoplasma Vacuolar Antigen. *Cell Rep.* 2015. **13:** 223–233.

45 **Avci, D. and Lemberg, M. K.**, Clipping or extracting: two ways to membrane protein degradation. *Trends Cell Biol.* 2015. **25:** 611–622.

46 **Oliveira, C. C., Querido, B., Sluijter, M., de Groot, A. F., van der Zee, R., Rabelink, M. J., Hoeben, R. C. et al.**, New role of signal peptide peptidase to liberate C-terminal peptides for MHC class I presentation. *J. Immunol.* 2013. **191:** 4020–4028.

47 **Oliveira, C. C. and van Hall, T.**, Alternative antigen processing for MHC class I: multiple roads lead to Rome. *Front Immunol.* 2015. **6:** 298.

48 **Romano, J. D., Sonda, S., Bergbower, E., Smith, M. E. and Coppens, I.**, Toxoplasma gondii salvages sphingolipids from the host Golgi through the rerouting of selected Rab vesicles to the parasitophorous vacuole. *Mol. Biol. Cell* 2013. **24:** 1974–1995.

49 **Cebrian, I., Croce, C., Guerrero, N. A., Blanchard, N. and Mayorga, L. S.**, Rab22a controls MHC-I intracellular trafficking and antigen cross-presentation by dendritic cells. *EMBO Rep.* 2016. **17:** 1753–1765.

50 **Lohi, O., Urban, S. and Freeman, M.**, Diverse substrate recognition mechanisms for rhomboids; thrombomodulin is cleaved by Mammalian rhomboids. *Curr. Biol.* 2004. **14:** 236–241.

51 **Friedmann, E., Hauben, E., Maylandt, K., Schleeger, S., Vreugde, S., Lichtenthaler, S. F., Kuhn, P. H. et al.**, SPPL2a and SPPL2b promote intramembrane proteolysis of TNFalpha in activated dendritic cells to trigger IL-12 production. *Nat. Cell Biol.* 2006. **8:** 843–848.

52 **Lawler, S. E., Speranza, M. C., Cho, C. F. and Chiocca, E. A.**, Oncolytic viruses in cancer treatment: a review. *JAMA Oncol.* 2016. https://doi.org/10.1001/jamaoncol.2016.2064

53 **Baird, J. R., Byrne, K. T., Lizotte, P. H., Toraya-Brown, S., Scarlett, U. K., Alexander, M. P., Sheen, M. R. et al.**, Immune-mediated regression of established B16F10 Melanoma by intratumoral injection of attenuated toxoplasma gondii protects against rechallenge. *J. Immunol.* 2013. **190:** 469–478.

54 **Baird, J. R., Fox, B. A., Sanders, K. L., Lizotte, P. H., Cubillos-Ruiz, J. R., Scarlett, U. K., Rutkowski, M. R. et al.**, Avirulent toxoplasma gondii generates therapeutic antitumor immunity by reversing immunosuppression in the ovarian cancer microenvironment. *Cancer Res.* 2013. **73:** 3842–3851.

55 **Schaeffer, M., Han, S. J., Chtanova, T., van Dooren, G. G., Herzmark, P., Chen, Y., Roysam, B. et al.**, Dynamic imaging of T cell-parasite interactions in the brains of mice chronically infected with Toxoplasma gondii. *J. Immunol.* 2009. **182:** 6379–6393.

56 **Donald, R. G., Carter, D., Ullman, B. and Roos, D. S.**, Insertional tagging, cloning, and expression of the Toxoplasma gondii hypoxanthine-xanthine-guanine phosphoribosyltransferase gene. Use as a selectable marker for stable transformation. *J. Biol. Chem.* 1996. **271:** 14010–14019.

Full correspondence: Dr. Nicolas Blanchard, CPTP INSERM U1043 - CHU Purpan - BP3028 – 31024 Toulouse Cedex 3 - France
e-mail: nicolas.blanchard@inserm.fr

Received: 7/12/2016
Revised: 21/3/2017
Accepted: 9/5/2017
Accepted article online: 15/5/2017

